Materials Science-Poland, Vol. 23, No. 2, 2005

Computer simulation study of solid C_{60} doped by hydrogen cyanide molecules

S. PAŁUCHA[1,2*], P. BROL[2], Z. GBURSKI[2]

[1]Department of Electrotechnology, Division of Computer Methods,
Silesian University of Technology, Krasińskiego 8, Katowice 40-019, Poland

[2]Institute of Physics, University of Silesia, Uniwersytecka 4, Katowice 40-007, Poland

Using the spherically averaged Girifalco potential model of interacting C_{60} fullerenes, the relaxation processes of hydrogen cyanide molecules embedded in a fullerene host has been simulated by the molecular dynamics method. The dynamics of molecules in the system has been studied by inspecting the calculated dipolar absorption spectrum and Arrheniu-like plot. Moreover, the translational and rotational correlation functions of HCN in fullerene environments have been calculated. Comparison with the bulk HCN systems at several temperatures was made.

Key words: *molecular dynamics; hydrogen cyanide; doped fullerene; dielectric relaxation*

1. Introduction

The properties of carbon allotropes with closed cage structures have been an active subject of research since the first experimental discovery in 1985 [1]. Subsequently, the structure and energies of fullerene balls have been intensively studied, both experimentally and theoretically. One of the most important endeavours is to try to change their mechanical and electronic properties by doping. In recent years, exohedrally and endohedrally doped fullerenes have been produced, using a variety of doping atoms or even small molecules. In the endohedral case, the molecule encloses the dopant species, isolating them from the outside. Many possible applications, for example the recently proposed electron -spin quantum computer [2], have been envisaged using these new systems. In the exohedral case, the dopant atoms (or molecules) are external, attached to the fullerene, as in the case of superconducting fullerides. The recently reported high-temperature superconducting fullerides [3] have turned scientists' attention to problems concerned with the stability of a doped fullerite matrix. The results obtained could be of value in areas of developing technology for the storage of poisons, such as HCN, inside fullerites.

* Corresponding author, e-mail: palucha@us.edu.pl

2. Potential model and the simulation performed

MD calculations for 216 HCN molecules doped inside 856 C_{60} molecules arranged in an FCC structure at the temperatures from 100 K to 1400 K and ρ = 1.73 g/cm^3 were carried out. The equation of motion was integrated with a leapfrog Verlet integration algorithm with coupling to the thermal bath (ensemble NVT) [4]. Because of the high frequency of the intramolecular vibrations, a small integration time step of 0.2 fs was employed which guarantees fluctuation of the potential energy of ~ 0.1%. A long MD run of 1×10^6 time steps (200 ps) was performed after an equilibration period of 20 ps. The HCN potential model is a three-point interaction site model with charges placed at the atomic centres of H, C, and N with the values of 0.119*e*, –0.333*e*, and 0.214*e*, respectively. In a classical mechanics approximation of intramolecular motion, the internal degrees of freedom are modelled by bond and angle potentials. The bonds and angles are normally constrained to fluctuate around some equilibrium value to avoid dissociation of the molecule. Such molecules allow the study of environmental effects on the intramolecular structure and vibrational frequency shifts can be determined, etc. As these are experimentally measurable data, potential models can be critically tested and new insights gained on the molecular nature of the phenomena. Molecular flexibility was introduced in the HCN potential by assuming that C–H and C–N vibrations were modelled by harmonic [4] potentials $V(r_{ij}) = 1/2\mathrm{k}(r_{ij} - r_0)^2$ with stretching force constants k_{CH} = 580N·m^{-1} (ν_{CH} = 3312 cm^{-1}) and k_{CN} = 1790 N·m^{-1} (ν_{CN} = 2089 cm^{-1}). The interatomic distances were r_0 = 1.06 Å and r_0 = 1.15 Å, respectively [5]. Periodic boundary conditions were used, and the long-ranged Coulombian interactions were computed with the Ewald summation method [4]. Samples of the trajectory were stored every 0.002 ps.

The interactions between HCN molecules have been modelled in terms of the Lennard–Jones potentials of the form $V(r_{ij}) = 4\varepsilon[(\sigma/r_{ij})^{12} - (\sigma/r_{ij})^6]$, where r_{ij} is the distance between the *i*-th and j-th atoms, ε is the minimum of the potential at the distance $2^{1/6}\sigma$. The following ε (in KJ/mol) and σ (in Å) have been taken [4]:

$$\varepsilon_{H-H} = 0.0715,\ \sigma_{H-H} = 2.81,\ \varepsilon_{N-N} = 0.3102,$$

$$\sigma_{N-N} = 3.35,\ \varepsilon_{C-C} = 0.4257,\ \sigma_{C-C} = 3.55.$$

The cross interactions were modelled with the Berthelod rules [4]. The interaction between two C_{60} molecules (Eq. (1)) was described according to the potential proposed by Girifalco [6], with the interactions values α and β equal 4.4775 kJ/mol and 0.0081 kJ/mol, respectively (the α and β coefficients being as in [6])

$$V_{C_{60}-C_{60}}(r) = -\alpha\left[\frac{1}{s(s-1)^3} + \frac{1}{s(s+1)^3} - \frac{2}{s^4}\right] + \beta\left[\frac{1}{s(s-1)^9} + \frac{1}{s(s+1)^9} - \frac{2}{s^{10}}\right] \quad (1)$$

where $s = r/\sigma_{C_{60}}$, with the diameter of the fullerene molecule $\sigma_{C_{60}} = 7.1$ Å.

Similarly, the interaction between C_{60} and HCN molecules has been taken into account, describing the interaction between a single atomic member of a C_{60} molecule and a gas atom in terms of the Lennard–Jones potential. Subsequent integration of the latter over the entire fullerene sphere results in the overall potential between the molecules given in [7].

$$V_{C_{60}\text{-site}}(r) = 60\left(\frac{c_6}{R^6}F_6(s) + \frac{c_{12}}{R^{12}}F_{12}(s)\right) \tag{2}$$

where

$$F_n = \frac{1}{s(n-2)}\left[(1-2s)^{2-n} - (1+2s)^{2-n}\right], \qquad 2R = \sigma_{C_{60}}, \qquad c_6 = -4\varepsilon_{\text{site-C}}\sigma_{\text{site-C}}^6$$

and

$$c_{12} = 4\varepsilon_{\text{site-C}}\sigma_{\text{site-C}}^{12}$$

with ε and σ presented previously (site ≡ H, C, N).

3. Results and discussion

Information about microscopic dynamics is usually provided in MD simulations by means of the atomic velocity autocorrelation function (VAF) $C_v(t)$ [4]. The expression for calculating VAF is

$$C_V(t) = \frac{\langle v(t)v(0)\rangle}{\langle v^2(0)\rangle} \tag{3}$$

Depending on the velocities chosen, any correlation function, i.e., for a particular direction (x, y, or z) or for a given species (hydrogen, carbon, or nitrogen) may be obtained. Here that for the C atom of the HCN molecule is presented. From the VAF we can compute the spectral densities which will be associated with the experimental Raman and infrared spectra. As an example in Fig. 1 the carbon VAFs for pure HCN and HCN doped in C_{60} at two temperatures 200 and 400 K is shown.

The shapes of the functions for the case of bulk HCN and C_{60} doped with HCN are noticeably different. In the doped case (Fig. 1b), the VAF decays to a negative value and reveals an oscillating long tail behaviour which is not observed in unconstrained HCN as shown in Fig 1a. Increasing the temperature in both systems shifts the VAFs to shorter times. The observed oscillation can be interpreted as a caging effect of the C_{60} host on HCN molecules. The spectral density $S(\omega)$ was analysed by

$$S(\omega) = \int_0^\infty dt\langle v(t)v(0)\rangle\cos(\omega t) \tag{4}$$

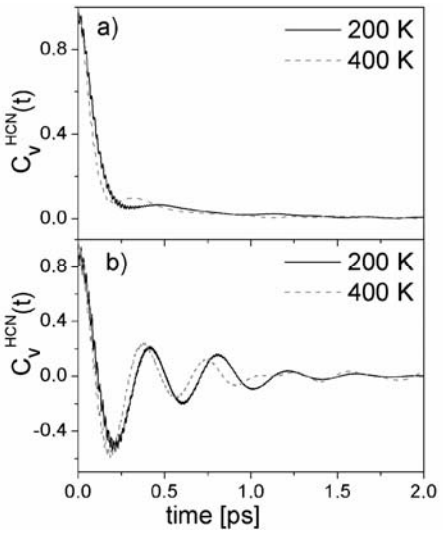

Fig. 1. Velocity autocorrelation function $C_v(t)$ calculated for two systems:
a) bulk HCN, b) HCN–C_{60} mixture

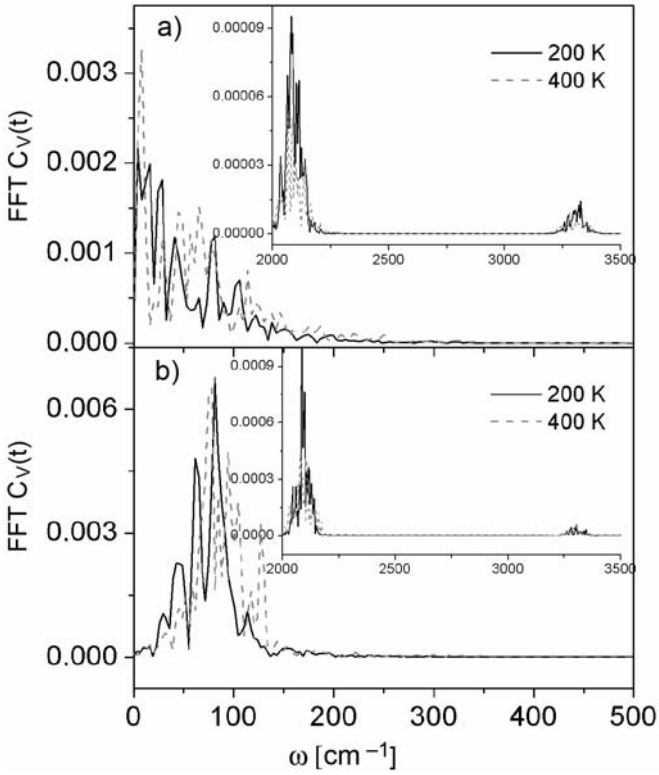

Fig. 2. Fourier transform of velocity correlation function $C_v(t)$ of HCN molecules obtained from: a) bulk HCN and b) HCN–C_{60} mixture at two temperatures 200 K and 400 K, respectively. The insets show the spectral densities at higher frequencies (mid-infrared) of stretching vibrations H–C and C–N, respectively

The Fourier transforms of the velocity autocorrelation functions for the hydrogen, carbon and nitrogen are related to the infrared spectrum [8]. The $S(\omega)$ have been calculated by numerical integration of the velocity autocorrelation functions calculated from MD simulations using standard FFT routines [9]. When generating spectra, a Hanning window was used and its width was the same as the sampling interval (20 fs). This choice of sampling interval corresponds to a Nyquist critical frequency of 8333 cm^{-1} and sets an upper bound on the frequency range over which the power spectra can be obtained. It is well known that the experimental frequency bands cannot be fully reproduced by classical simulations and this paper is restricted to a qualitative analysis mainly focused on the frequency shifts. The nitrogen spectral densities (far-infrared) found for two temperatures are plotted in Fig. 2 and are compared for the doped C_{60} and bulk HCN case.

In general, the rise of temperature produces a weakening in the intensity of frequency modes. The low frequency spread around 50 cm^{-1} in bulk HCN changed to narrower features shifted to higher frequencies around 80 cm^{-1}. This behaviour is associated with the restricted cage motions typical for dense liquids. In both cases, the intramolecular vibrational (mid-infrared) modes for HCN corresponding to stretching frequencies around 2089 cm^{-1} (H-C) and 3312 cm^{-1} (C-N), are clearly seen (see insets in Fig. 2a, b).

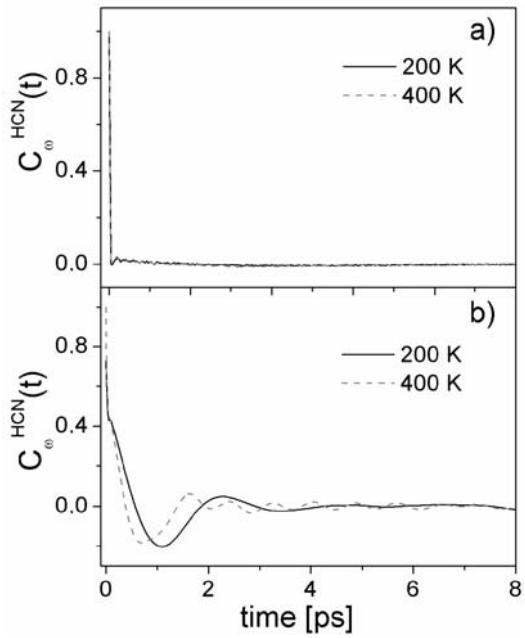

Fig. 3. Angular velocity autocorrelation function $C\omega(t)$ calculated for two systems: a) bulk HCN, b) HCN–C_{60} mixtures

Insight into rotational motion is given by the rotational relaxation functions. One of them is the angular velocity autocorrelation function (AVAF) $C\omega(t)$ which is presented in Fig. 3. The expression for calculating AVAF is

$$C_\omega(t) = \frac{\langle \omega(t)\omega(0)\rangle}{\langle \omega^2(0)\rangle} \tag{5}$$

Firstly it must be noted that at very short times AVAF in bulk HCN (Fig. 3a) decays rapidly to values near zero and remains in a long-time tail. The main difference arising from doping C_{60} with HCN is the occurrence of negative values in AFAF at short-times (up to 2 ps). The corresponding Fourier transforms are presented in Fig. 4.

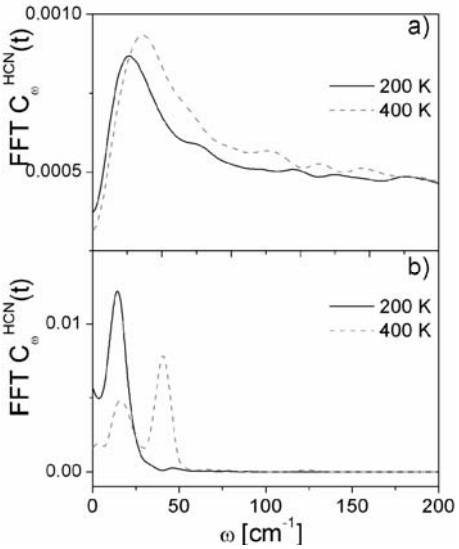

Fig. 4. Fourier transform of angular velocity correlation function $C\omega(t)$ obtained from: a) HCN and b) HCN–C_{60} mixture at two temperatures 200 K and 400 K, respectively

In both cases the influence of increasing temperature shifts the peaks to higher frequency values. The fast unconstrained reorientation located near 52 cm^{-1} at T = 200 K moves to 73 cm^{-1} at T = 400 K in bulk HCN. However, in HCN doped C_{60} the well pronounced maximum at 15 cm^{-1} shifts its location to 17 cm^{-1} and diminishes at higher temperatures. Moreover, at T = 400 K new maxima are developed at 41 cm^{-1}.

Now consider the relaxation processes of polar impurities (HCN) in the fullerene environment in terms of the dielectric formalism. In experiments one can measure the frequency dependency of permittivity $\varepsilon'(\omega)$ and loss $\varepsilon''(\omega)$, which are the real and imaginary parts of the dielectric function $\varepsilon(\omega) = \varepsilon'(\omega) + i\varepsilon''(\omega)$. The data obtained can be compared to many theoretical models. For example, the single-relaxation-time Debay model [10] described by the following equation for a complex dielectric function:

$$\frac{\varepsilon^*(\omega) - \varepsilon_\infty}{\varepsilon_0 - \varepsilon_\infty} = \frac{1}{1 + (i\omega\tau_D)^2} \tag{6}$$

where $\omega = 2\pi\nu$ is the angular frequency, ε_∞ is the intrinsic permittivity, ε_0 is the static permittivity and τ_D is the relaxation time parameter. Moreover, there are empirical expressions such as that originally proposed by Havriliak and Negami [11]:

$$\frac{\varepsilon^*(\omega)-\varepsilon_\infty}{\varepsilon_0-\varepsilon_\infty}=\left(1+\left(i\omega\tau_D\right)^m\right)^{-n/m} \tag{7}$$

where the parameter ω, ε_∞, ε_0, and τ_D have the same meaning as stated earlier. Dissado and Hill [12] developed the concept of clusters and the various charge or dipolar transitions being divided into intra-cluster ones occurring within clusters and inter-clusters transitions occurring between the clusters. A cluster is defined as an assembly of molecules surrounding a defect which vibrates coherently with slightly modified frequencies with respect to the frequencies of the perfect lattice. The degree of coherence of these motions is measured by an index $1-n$. The case of $1-n$ approaching unity implies a high degree of coherence, similar to that which might arise in strongly interacting defects/lattice systems. Similarly, the case of $1-n$ approaching zero denotes incoherent cluster oscillations with slight distortion of the lattice by the defect. The evolution of cluster relaxations now proceeds through what is termed inter-cluster transitions, where adjacent clusters exchange oscillating molecules. This process is characterized by a parameter m which, in relation to this process, plays a role analogous to that of n for the intra-cluster transitions. The shape of the dielectric response depends on the long-range inter-cluster correlations at low frequencies ($\omega << \omega_D$) and on the short-range intra-cluster dynamics at high frequencies ($\omega >> \omega_D$). The basic assumption of the Dissado–Hill approach is the self-similarity in the energy redistributions within and among clusters (short-range and long-range interactions). The parameter m is related to the degree of inter-cluster correlation, while the parameter n reflects the local intra-cluster dynamics.

A connection between the measurable quantity $\varepsilon(\omega)$ and the relaxation function $C_M(t)$ can be introduced. Using the Fröhlich theory of dielectrics [13], the permittivity and dielectric loss can both be connected with this relaxation function:

$$\begin{aligned}\varepsilon'(\omega)&=\varepsilon_0-(\varepsilon_0-1)\,\omega\int_0^\infty C_M(t)\sin(\omega t)dt\\ \varepsilon''(\omega)&=(\varepsilon_0-1)\,\omega\int_0^\infty C_M(t)\cos(\omega t)dt\end{aligned} \tag{8}$$

where $C_M(t)=\langle\mathbf{M}(t)\cdot\mathbf{M}(0)\rangle\cdot\langle\mathbf{M}(0)\cdot\mathbf{M}(0)\rangle^{-1}$ is a correlation function of macroscopic dipole moment $\mathbf{M}(t)=\sum_{i=1}^{n}\mathbf{m}_i(t)$; $\mathbf{m}_i$ is dipole moment of i-th molecule and n is the total number of HCN molecules.

In Figures 5a, b, the imaginary part of the dielectric response of pure HCN and HCN in a fullerene environment in log scale is presented.

The $\varepsilon''(\omega)$ peaks are located between 1 and 30 cm^{-1}. In the case of HCN doped C_{60} the dielectric loss peaks change their magnitude and alter slightly the shape and fre-

quency positions from 20 cm^{-1} to 3 cm^{-1}. These features depend on temperature. The obtained data were fitted using Eq. (7). The fitted parameter m and $1 - n$ for the high- and low-frequency exponents are also presented in Fig. 5. These values are typical of polar interaction. Note, that doping HCN into C_{60} results in an increase of the $1 - n$ value, which suggests more coherent cluster oscillations following the interpretation of the Havriliak and Negami model. An Arrhenius plot of the frequency position of the dielectric loss peaks shown in Fig. 5 is presented in Fig 6.

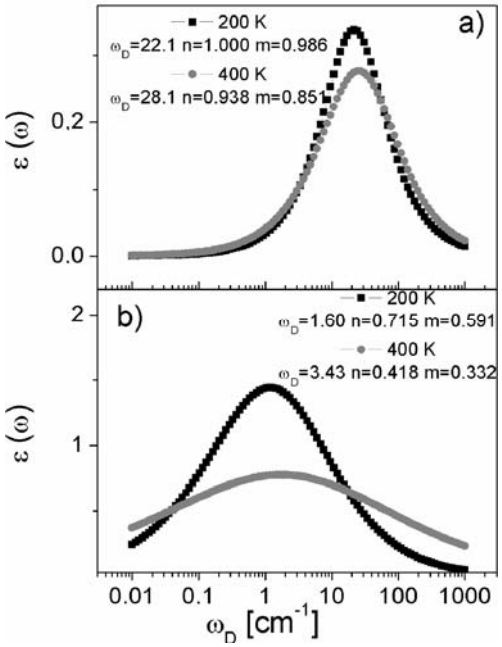

Fig. 5. Frequency dependence of the imaginary part of dielectric function obtained from: a) HCN, b) HCN–C_{60} mixture at two temperatures 200 K and 400 K, respectively

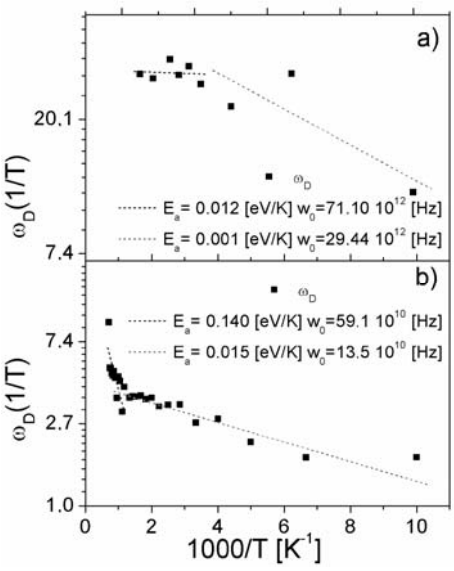

Fig. 6. Arrhenius plot of the position of the dielectric loss peak frequency obtained from a) HCN system and b) C_{60}–HCN mixtures

It was found that the peaks are indeed temperature activated with a functional dependence:

$$\omega_D = \omega_0 \exp\left(-\frac{E_a}{k_B T}\right) \tag{9}$$

where E_a is the activation energy, and ω_0 is the frequency prefactor. In general, two regions connected with low- and high-temperature behaviour of ω_D could be approximated. From Fig. 6a (pure HCN) it was found that the activation energy of the loss peak below the phase transition at $T = 260$ K is 0.001 eV, whereas the activation energy E_a above the phase transition is 0.012 eV. In the HCN–C_{60} mixture, the activa-

tion energies E_a are 0.015 eV/K and 0.14 eV/K with the phase transition at $T = 700$ K. In the pure HCN molecules the activation energy is an order of magnitude smaller than the one for HCN located inside the fullerene matrix. This means that in the former system the HCN molecules start rotating freely, while in the latter the rotation of HCN in C_{60} system is constrained. In both analyzed systems the frequency prefactor ω_0 is within the phonon frequency range 10^{10}–10^{12} Hz.

4. Conclusion

In this study, the molecular dynamics technique was used to simulate the C_{60}–HCN system. This system has been systematically investigated and the rotational behaviour was analysed. Two areas were found (see Fig. 6); below 700 K the rotation of HCN is hindered, for higher temperatures it is almost undisturbed. Substantial differences in the dynamics of pure HCN and HCN doped C_{60} are reported.

References

[1] KROTO H.W., HEATH J.R., O'BRIEN S.C., CURL R.F., SMALLEY R.E., Nature, 318 (1985), 162.
[2] HERNEIT W, Phys. Rev. A, 65 (2002), 032322.
[3] DRESSELHAUS M.S., DRESSELHAUS G., EKLUND P.C., *Science of Fullerenes and Carbon Nanotubes*, Academic Press, New York, 1996.
[4] ALLEN M.P., TILDESLEY D.J., *Computer Simulations of Liquids*, Oxford University Press, Oxford, 1989.
[5] HERZBERG G., *Molecular Spectra and Molecular Structure*, Vol. II, p. 173, D. van Nostrand, New York, 1966.
[6] GIRIFALCO L.A., J. Phys. Chem., 95 (1992), 5370.
[7] BRETON J., GONZALES-PLATAS J., GIRARDET C., J. Chem. Phys., 99 (1993), 4036.
[8] MARTÍ J., GUÀRDIA E., PADRÓ J.A., J. Chem. Phys., 101, (1994), 10883.
[9] PRESS W.H., FLANNERY B.P., TEUKOLSKY S.A., VETTERLING W.T., *Numerical Recipes in Fortran*, Cambridge University Press, Cambridge, 1992.
[10] JONSCHER A.K., *Dielectric Relaxation in Solids*, Chelsea Dielectrics, London, 1983.
[11] HAVRILIAK S., NEGAMI S., Polymer 8 (1967), 161.
[12] DISSADO L.A., HILL R.M., Chem. Phys., 111 (1987), 193.
[13] FRÖHLICH H., *Theory of Dielectrics*, Oxford University Press, London, 1958.

Received 7 September 2004
Revised 21 December 2004